MR Determination of Hippocampal Volume: Comparison of Three Methods

Dominique Hasboun, Martine Chantôme, Abderrezak Zouaoui, Mokrane Sahel, Michèle Deladoeuille, Nader Sourour, Michel Duyme, Michel Baulac, Claude Marsault, and Didier Dormont

PURPOSE: To determine whether measurements of the volume of the hippocampal formation obtained from a three-dimensional acquisition not perpendicular to the hippocampus are statistically different from those obtained from a perpendicular acquisition. **METHODS:** Both hippocampi were studied in 10 healthy volunteers with two three-dimensional acquisitions, allowing three different volume-calculation protocols: (*a*) on sections from a coronal 3-D acquisition not perpendicular to the axis of the hippocampal formation (NOPERP protocol), (*b*) on sections obtained with the same acquisition but reformatted perpendicular to the axis of the hippocampal formation (REFOR protocol), and (*c*) on sections from a coronal 3-D acquisition perpendicular to the axis of the hippocampal formation (PERP protocol) obtained with the patient's head tilted backward. To obtain measurements of the volume of the hippocampal formations, an accurate 3-D processing technique was used to segment the hippocampus. In all subjects, two hippocampal formation right-left asymmetry indexes were calculated by using each of the three protocols. **RESULTS:** For the right hippocampus, the mean volume was 3.42 cm^3 (NOPERP protocol), 4.18 cm^3 (REFOR protocol), and 3.91 cm^3 (PERP protocol). For the left hippocampus, the mean volume was 3.29 cm^3 (NOPERP protocol), 4.02 cm^3 (REFOR protocol), and 3.74 cm^3 (PERP protocol). For both hippocampi, the differences of the mean volumes were significant between each protocol. However, for both hippocampi, a high correlation was observed between volumes obtained with the different protocols. For the two asymmetry indexes, there were no significant differences for the means obtained with the three protocols. **CONCLUSION:** With the use of 3-D acquisitions in the study of hippocampal formation biometry, different procedures lead to significant variations in the absolute values of the volume of the hippocampal formation. However, there is a strong correlation between the results obtained by each method.

Index terms: Brain, magnetic resonance; Brain, measurements; Hippocampus

AJNR Am J Neuroradiol 17:1091–1098, June 1996

Magnetic resonance (MR) imaging has been used in studies of the hippocampal formation and in amygdala biometric studies for several years. The biometric data are useful for evaluating selective hippocampal atrophy in patients with intractable partial seizures (1–6), Alzheimer-type dementia (7), amnesic syndromes (8), or schizophrenia (9, 10). Obvious hippocampal atrophy seen on MR images corresponds to severe neuronal loss (11–13). Thus, early diagnosis depends on the ability to detect small variations in hippocampal volume. Different MR sequences have been used to evaluate the volume of the hippocampal formation, and technical progress has allowed reduction of section thickness. At present, a technique using three-dimensional gradient-echo acquisition allows very thin contiguous sections to be obtained (4, 5, 9, 12, 14–17). In addition, the use of an independent workstation with 3-D software has improved data processing. However, some problems concerning the use of 3-D acquisition for measuring the volume of the hippocampal formation still exist. Many authors (7,

Received August 31, 1995; accepted after revision January 18, 1996.

From the Departments of Neuroradiology (D.H., A.Z., M.S., M.De., N.S., C.M., D.D.) and Neurology (D.H., M.B.), Pitié-Salpêtrière Hospital University Paris VI, and the Department of Biological Anthropology and Genetic Epidemiology, INSERM U155 (M.C., M.Du.), Paris, France.

Address reprint requests to Didier Dormont MD, Department of Neuroradiology, Pitié-Salpêtrière Hospital, 83 Boulevard de L'Hôpital, 75651 Paris, Cedex 13 France.

AJNR 17:1091–1098, June 1996 0195-6108/96/1706–1091

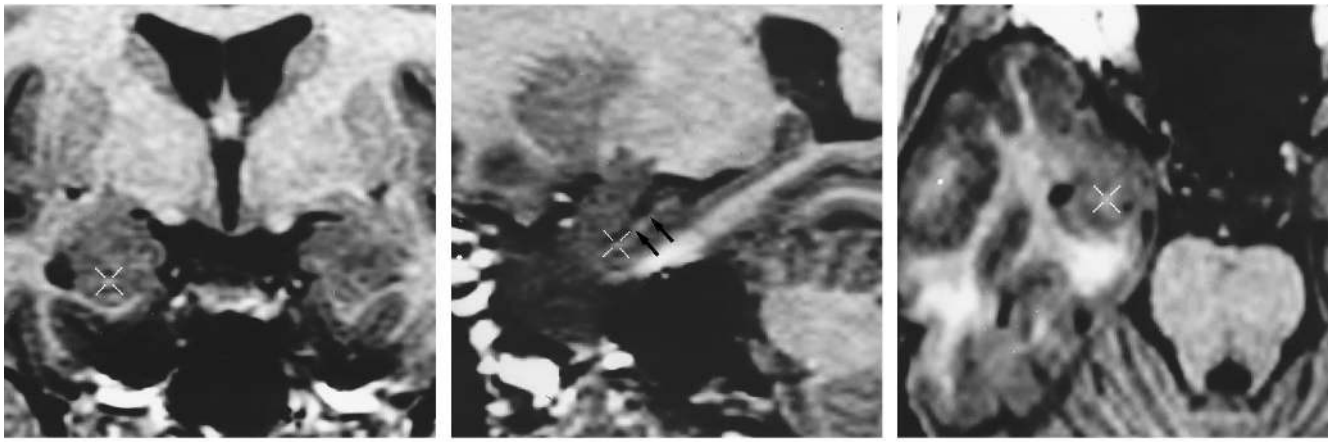

Fig 1. Image processing. The 3-D cursor guides the complex separation of the hippocampus from the amygdala in the coronal plane (*A*), checking its location in the sagittal (*B*) and the axial (*C*) planes. The alveus, a thin structure of white matter separating the pes hippocampus from the amygdala, is particularly well seen in the sagittal plane (*arrows* in *B*).

18, 19) state that, in measurements of hippocampal volume, acquisitions in the plane perpendicular to the axis of the hippocampus is mandatory. This is easily accomplished with the use of two-dimensional spin-echo or inversion-recovery sequences; but, on most MR imaging units, 3-D oblique acquisitions are impossible. Although this can be overcome by modifying the patient's position, the angle at which the head must be tilted to obtain an acquisition perpendicular to the axis of the hippocampal formation is very uncomfortable and cannot be used routinely in clinical practice.

The purpose of this study was to ascertain whether measurements of the volume of the hippocampal formation obtained from a 3-D acquisition not perpendicular to the axis of the hippocampal formation were significantly different from those obtained from a perpendicular acquisition and to evaluate whether, in 3-D nonperpendicular acquisitions, there were discrepancies in the volume measurements between nonreformatted and reformatted sections.

Subjects and Methods

Ten healthy volunteers were studied. The subjects included five men and five women who were 22 to 47 years old (mean, 29 years; SD, 6.7). They were neurologically intact and had no systemic disease.

MR imaging was performed on a 1.5-T unit. We performed two volumetric acquisitions for each subject, one in a coronal plane (not perpendicular to the hippocampal formation) and the other in a plane perpendicular to the axis of the hippocampal formation. During the latter acquisition, the subject was placed supine within the magnet, and the head was tilted backward so that an imaginary line joining the lips and the external auditory canal was perpendicular to the examination table. A 600/11/1 (repetition time/echo time/excitations) sagittal spin-echo sequence was obtained to verify that the hippocampus was perpendicular to the coronal plane. If necessary, the head orientation was adjusted to position the hippocampus properly. The volumetric acquisitions were obtained with the spoiled gradient recalled acquisition in a steady state (GRASS) sequence. Parameters of the sequence were 23/5/1; flip angle was 35°; field of view was 22 cm, and matrix size was 256 × 192. One hundred twenty-four contiguous sections were obtained of the entire head. Section thickness was 1.5 mm.

Each acquisition was transferred to a workstation. Volumetric measurements were performed using the 3-D option software. A 3-D model of the head was obtained from the 124 sections by using a low threshold of 25 and a high threshold of 400 (arbitrary units). These values limited the range of voxel intensity used in generating the 3-D model. The model was seen in four synchronized windows: 3-D, coronal, axial, and sagittal. The width of the gray scale and the level of the four windows were adjusted visually, and images were magnified by a factor of 3.4. Processing was performed with a 3-D mouse-driven cursor, which appeared simultaneously at the same location in all the active visualized planes. This device permits the operator to know the exact anatomic location of the cursor and, in particular, to differentiate the most anterior part of the hippocampus from the amygdala (Fig 1). Three segmentations of the hippocampal formation allowing three different volumetric calculations were performed in all subjects as follows: (*a*) volume was measured on sections of the coronal 3-D acquisition that was not perpendicular to the axis of the hippocampal formation (NOPERP protocol) (Fig 2); (*b*) using the same acquisition, segmentation was performed on sections reformatted (REFOR protocol) in the plane perpendicular to the axis of the hippocampal

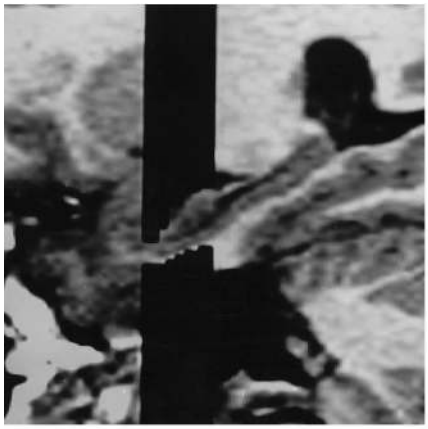

2

Fig 2. Image processing, right hippocampus in healthy volunteer: hippocampal segmentation on sections obtained from the acquisition not perpendicular to the hippocampus (NOPERP protocol).

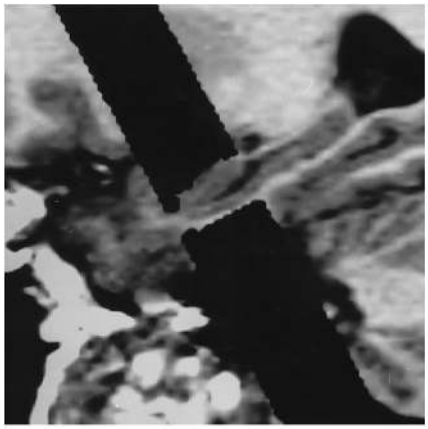

3

Fig 3. Image processing, right hippocampus in healthy volunteer: hippocampal segmentation on reformatted coronal sections (perpendicular to the hippocampus) obtained from the nonperpendicular acquisition (REFOR protocol).

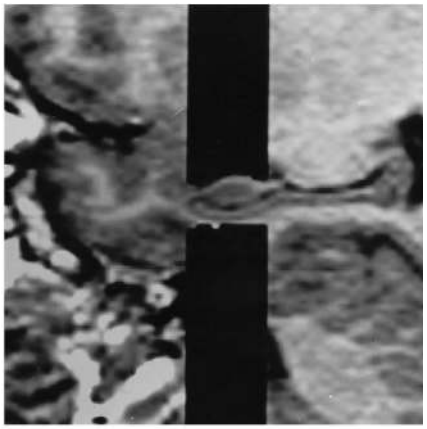

4

Fig 4. Image processing, right hippocampus in healthy volunteer: hippocampal segmentation on sections obtained from the acquisition perpendicular to the hippocampus (PERP protocol).

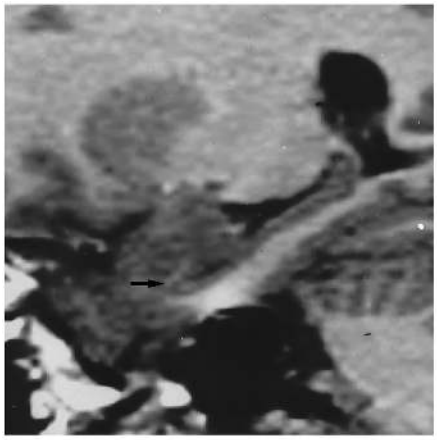

A

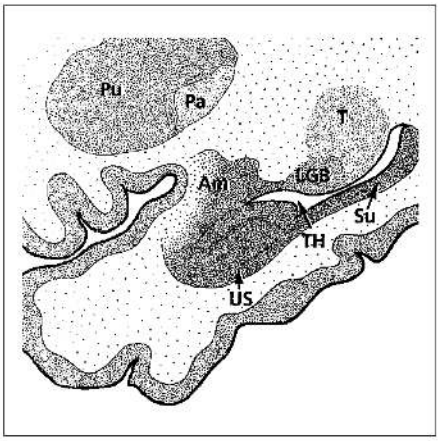

B

Fig 5. *A*, Spoiled GRASS image reformatted in the sagittal plane shows the anterior limit of the hippocampal segmentation just rostral to the uncus (*arrow*).

B, Anatomic drawing at the same level shows the major anatomic structures related to the hippocampus. *Am* indicates amygdala; *LGB*, lateral geniculate body; *Pa*, pallidum; *Pu*, putamen; *Su*, subiculum; *T*, thalamus; *TH*, temporal horn; and *US*, uncal sulcus.

formation (Fig 3); the plane perpendicular to the hippocampus was determined from the sagittal reformatted view centered on the right hippocampus; and (*c*) segmentation was performed on the coronal 3-D acquisition obtained with the patient's head positioned in such a way that the acquisition plane was perpendicular (PERP protocol) to the axis of the hippocampal formation (Fig 4). The segmentations were performed by two different operators. Total time for the segmentation of one hippocampus with one protocol was approximately 40 minutes.

The measurements included the entire rostrocaudal extent of the hippocampus (eg, CA-1 through CA-4 sectors of the hippocampus proper, the dentate gyrus, the alveus, the fimbria, and a part of the subiculum). The hippocampus was progressively segmented rostrocaudally. The boundaries were outlined in the coronal plane. The increment between two segmentation planes was 2 mm. This increment was slightly greater than the section thickness, but it could be obtained with the 3-D software (with sections parallel to the acquisition or with reformatted sections) and it was chosen to shorten the total time needed for segmentation. The first section, checked in the sagittal window (Fig 5), was located just 2 mm caudal to the plane intersecting the most anterior extension of the alveus, just rostral to the uncus. The most accurate anterior limit was searched with the 3-D cursor interactively in the coronal, sagittal, and axial planes. Anatomic landmarks of the hippocampal formation were defined at the level of the head, body, and tail of the hippocampus, as described below.

Hippocampal Head

Dorsally and laterally, the alveus provides a landmark for the hippocampal head. It allows the examiner to differentiate the hippocampus from the overlying amygdala with the 3-D cursor. At this level, the hippocampus has a characteristic triangular shape (Fig 6). The location of the cursor in the coronal plane was always simultaneously

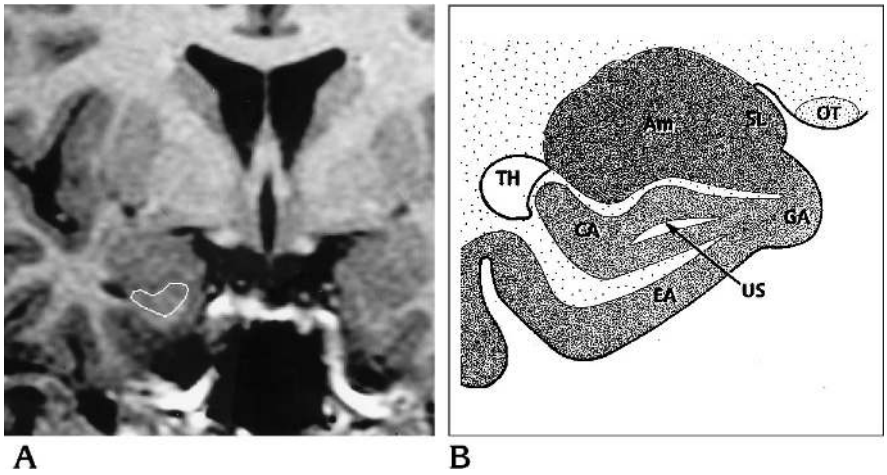

Fig 6. *A*, Spoiled GRASS coronal image (PERP protocol) shows the landmarks of the rostral part of the hippocampal head.

B, Anatomic drawing at the same level shows the close amygdalohippocampal relations. *Am* indicates amygdala; *CA*, cornu Ammonis; *EA*, entorhinal area; *GA*, gyrus ambiens; *OT*, optical tract; *SL*, semilunar gyrus; *TH*, temporal horn; and *US*, uncal sulcus.

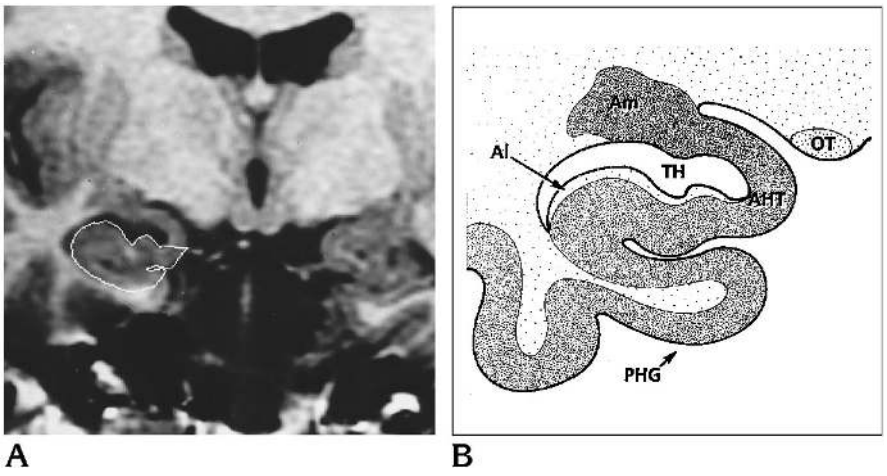

Fig 7. *A*, Spoiled GRASS coronal image (PERP protocol) shows the landmarks of the hippocampal head at the level of the digitations.

B, Anatomic drawing at the same level shows the reduction of the amygdalohippocampal relations. *AHT* indicates amygdalohippocampal transition area; *Al*, alveus; *Am*, amygdala; *OT*, optical tract; *PHG*, parahippocampal gyrus; and *TH*, temporal horn.

checked in the sagittal plane. More caudally, at the level of the digitations of the pes hippocampus, the temporal horn appears and enhances this dorsal limit. At this level, the medial part of the hippocampal head merges with the amygdala at the level of the amygdalohippocampal transition area (Fig 7). We traced a horizontal line along the extent of the alveus to cut this amygdalohippocampal area. The ventral limit was clearly defined by the gray–white matter junction between the white matter of the entorhinal cortex and the subiculum. Medially, the boundary of the hippocampal head was limited by the uncal sulcus and ambient fissure. The intralimbic gyrus was outlined in the most caudal planes of the pes hippocampus.

Hippocampal Body

The hippocampal body was easier to outline (Fig 8): dorsally and laterally we included the alveus overlying the cornu Ammonis. This boundary is well defined in the floor of the temporal horn. The fimbria was included in the measurements. Medially, we chose an arbitrary landmark located in the middle of the subiculum. The dentate gyrus located between the fimbria and the hippocampal fissure was included. Ventrally and laterally, the white matter was well distinguished from the subiculum and from CA-1.

Hippocampal Tail

Dorsally and laterally, the alveus was outlined up to the origin of the crus fornices medially, which was cut along the extent of the alveus (Fig 9). The medial landmark was an arbitrary vertical line traced at the level of the medial limit of the hippocampal sulcus. The section showing the entire length of the crus fornices was considered the posterior limit of the hippocampal tail and it was not included in the segmentation process.

After the segmentation process, the hippocampus was portrayed on a 3-D–rendered image (Fig 10) and the numeric values of the volume obtained by the 3-D software were also displayed. Both hippocampi were studied in all subjects. Using each protocol, we calculated two hippocampal asymmetry indexes for each subject. The first index (R1), was computed as follows:

$$R1(\%) = \frac{100 \times (R - L)}{Max\ (R, L)}$$

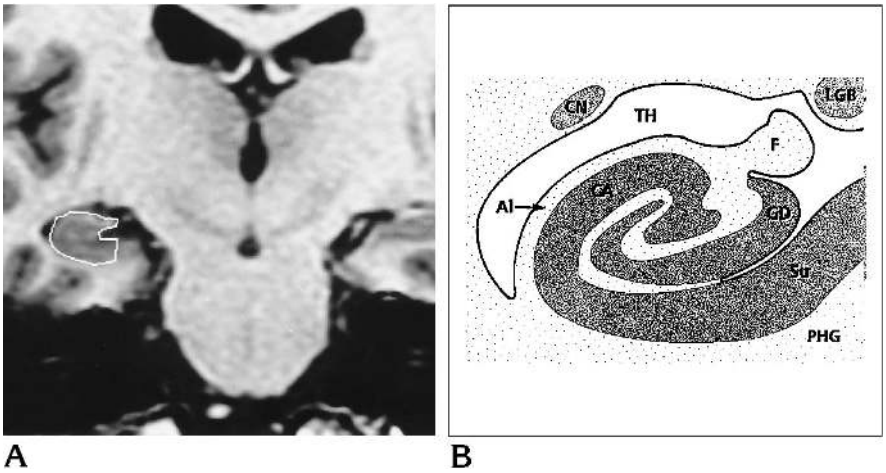

Fig 8. *A*, Spoiled GRASS coronal image (PERP protocol) shows the landmarks of the hippocampal body.

B, Anatomic drawing at the same level. *Al* indicates alveus; *CA*, cornu Ammonis; *CN*, caudate nucleus; *F*, fimbria; *GD*, gyrus dentatus; *LGB*, lateral geniculate body; *PHG*, parahippocampal gyrus; *Su*, subiculum; and *TH*, temporal horn.

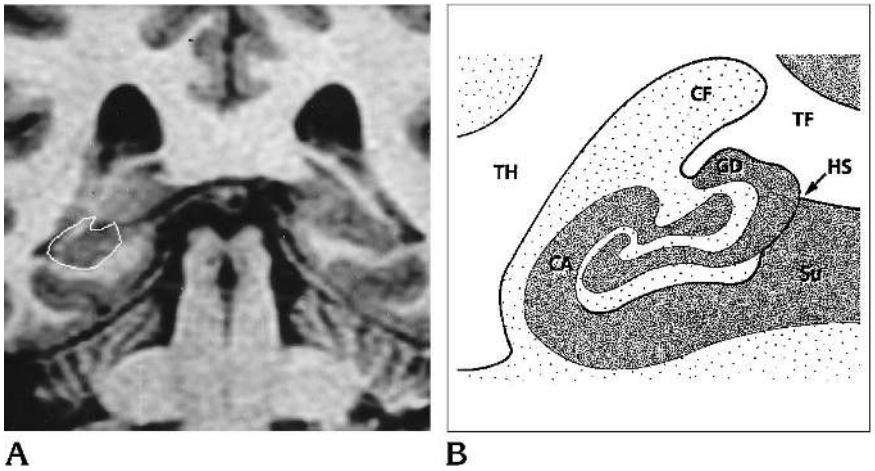

Fig 9. *A*, Spoiled GRASS coronal image (PERP protocol) shows the landmarks of the hippocampal tail.

B, Anatomic drawing at the same level. *CA* indicates cornu Ammonis; *CF*, crus fornices; *GD*, gyrus dentatus; *HS*, hippocampal sulcus; *Su*, subiculum; *TF*, transverse fissure; and *TH*, temporal horn.

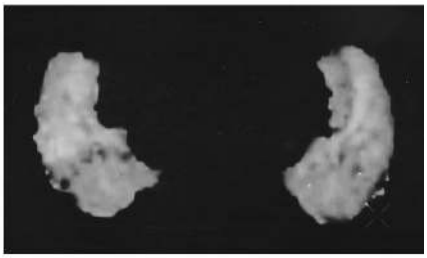

Fig 10. Anterosuperior view (45°) of the 3-D right and left hippocampi obtained after the segmentation process and the extraction from the brain (PERP protocol).

where *R* and *L* are, respectively, the values of the right and left hippocampus volumes and *Max(R, L)* is the highest value among the right and the left volumes (1). The second index (R2) was computed as follows:

$$R2(\%) = \frac{100 \times (R - L)}{\left(\frac{R + L}{2}\right)}$$

(20). The statistical analysis included the calculation of the Pearson product-moment correlation between each protocol and a *t* test for dependent samples to test the difference of means between each protocol.

Interobserver reproducibility was studied on both hippocampi for the 10 subjects with the REFOR protocol and was very elevated. Variance analysis showed that, for the right hippocampi, 95.3% of the variance was due to the true variance of the hippocampi; for the left, it was 92.7%. Thus, only 4.7% of the variance for the right hippocampi and 7.3% for the left hippocampi was due to interobserver variability.

Results

Values of hippocampal volumes and asymmetry indexes obtained with the three measurement protocols in the 10 subjects are described successively in the following sections.

Right Hippocampus

The mean volumes of the right hippocampus were 3.42 cm^3 (NOPERP protocol), 4.18 cm^3 (REFOR protocol), and 3.91 cm^3 (PERP protocol) (Table). The difference of the mean volume of the right hippocampus was significant ($P < .001$) between NOPERP and PERP protocols,

Mean values of right and left hippocampal volumes, R1 and R2 ratios obtained with the three different protocols

Protocol	R Hippocampus, mean ± SD	L Hippocampus, mean ± SD	R1 (%), mean ± SD	R2 (%), mean ± SD
NOPERP	3.42 cm^3 ± 0.49	3.29 cm^3 ± 0.63	4.3 ± 6.0	4.57 ± 6.5
REFOR	4.18 cm^3 ± 0.53	4.02 cm^3 ± 0.74	4.4 ± 6.5	4.65 ± 6.8
PERP	3.91 cm^3 ± 0.53	3.74 cm^3 ± 0.64	4.6 ± 6.0	4.91 ± 6.4

Note.—NOPERP indicates acquisition not perpendicular to axis of hippocampal formation; REFOR, same acquisition, sections reformatted perpendicular to axis; and PERP, coronal 3-D acquisition perpendicular to axis. See "Hippocampal Tail" section for formulations of asymmetry indexes R1 (%) and R2 (%).

between REFOR and PERP protocols, and between NOPERP and REFOR protocols. The difference between mean volumes of the right hippocampus computerized with PERP and NOPERP protocols (0.49 cm^3) was higher than the difference of mean volumes calculated with REFOR and PERP protocols (0.27 cm^3), but this latter result was not statistically significant ($P = .06$). The volumes of the right hippocampus were significantly correlated ($P < .001$) between NOPERP and PERP protocols ($r = .91$), REFOR and PERP protocols ($r = .95$), and NOPERP and REFOR protocols ($r = .91$).

Left Hippocampus

The mean volumes of the left hippocampus were 3.29 cm^3 (NOPERP protocol), 4.02 cm^3 (REFOR protocol), and 3.74 cm^3 (PERP protocol) (Table). The difference of the mean volume of the left hippocampus was significant ($P < .001$) between NOPERP and PERP protocols, between REFOR and PERP protocols, and between NOPERP and REFOR protocols. The difference between left hippocampus mean volumes computerized with PERP and NOPERP protocols (0.45 cm^3) was higher than the difference of mean volumes calculated with REFOR and PERP protocols (0.28 cm^3), but again this latter result was not statistically significant ($P = .18$). The volumes of the left hippocampus were significantly correlated ($P < .001$) between NOPERP and PERP protocols ($r = .91$), REFOR and PERP protocols ($r = .98$), and NOPERP and REFOR protocols ($r = .95$).

Asymmetry Indexes

The mean R1s were 4.3% (NOPERP protocol), 4.4% (REFOR protocol), and 4.6% (PERP protocol) (Table). The difference of the mean ratio R1 was not significant between NOPERP and PERP protocols ($P = .86$), between REFOR and PERP ($P = .80$), and between NOPERP and REFOR ($P = .97$). The difference between PERP-NOPERP (0.29%) and between PERP-REFOR (0.24%) was not significant ($P = .80$). The correlations of the R1 asymmetry indexes between each protocol were all significant ($P < .05$).

The mean R2s were 4.57% (NOPERP protocol), 4.65% (REFOR protocol), and 4.91% (PERP protocol). The difference of the mean ratio R2 was not significant between NOPERP and PERP ($P = .84$), between REFOR and PERP ($P = .79$), and between NOPERP and REFOR ($P = .96$). The difference PERP-NOPERP (0.34%) and between PERP-REFOR (0.26%) was not significant ($P = .80$). The correlations of the R2 asymmetry indexes between each protocol were all significant ($P < .05$).

Discussion

The in vivo biometry of the hippocampus has been applied to the study of temporal lobe epilepsy (1–6, 21, 22), Alzheimer disease (7), amnesia (8, 23), and schizophrenia (9, 10). Progress regarding biometry techniques in the hippocampus has involved image acquisition and data processing (5, 7–9, 17, 23, 24–38).

At present, many researchers are using 3-D acquisition sequences (5, 9, 17, 31), which can be successively transferred on a workstation to permit segmentation and volume calculation. All authors (4, 5, 9, 17) report segmentation of the hippocampal formation in the coronal plane without the use of any 3-D control. However, these 2-D segmentations have important limitations, principally concerning the anatomic identification of complex structures. For example, to separate the pes hippocampus (which is one of the most voluminous parts of the hippocampal formation) from the overlying amygdala is very difficult and sometimes impossible with the use of 2-D processing software. Some authors (8, 17, 23, 37) have preferred to exclude this region despite its significant volume.

Our study shows that these anatomic problems can be solved by means of 3-D processing of the data. The major benefit of 3-D processing is the 3-D cursor, which enables simultaneous identification of an anatomic structure in three orthogonal reformatted planes. With the use of 3-D processing, the major problem related to the complex anatomy of the pes hippocampus is easily solved. This is useful for the small anatomic structures (such as the alveus and the fimbria), because each point of the structure, located in the coronal plane, can be checked and simultaneously displayed in the sagittal and axial planes. Thus, the rostrocaudal and mediolateral extents of the hippocampal formation are respectively displayed in the sagittal and axial planes. The major benefit of 3-D processing is in resolving anatomic ambiguities; for example, when a boundary is not clear in the coronal plane, it can be examined by looking at it simultaneously in the other planes.

Using this method of hippocampal segmentation, we made three measurements of the volume of the hippocampal formation in each subject in order to evaluate and compare the different results. It is commonly accepted that all volume measurements of the hippocampal formation should be performed in a plane perpendicular to its axis because of problems related to partial volume effects (8). However, with most MR units, 3-D oblique acquisitions are not available. Some authors have used one of the three protocols of measuring the volume of the hippocampal formation that we used (5, 9, 14–17, 38). However, a study comparing the results of the different protocols is not available. The aim of our study was to compare the results of these three protocols. In our series, acquisition and measurements performed directly perpendicular to the hippocampal formation (PERP protocol) were considered as the reference because it avoided the possibility of introducing errors caused by partial volume effects (as with the NOPERP protocol) or by interpolated voxel values (as with the REFOR protocol). Our study shows that, even with a small group of 10 subjects, there was a significant difference between the results obtained with each protocol. The smallest values of the volume of the hippocampal formation were obtained with the NOPERP protocol; the highest values with the REFOR protocol. In all subjects, volumes obtained with the reference protocol (PERP protocol) were always between those obtained with the NOPERP and REFOR protocols. Our results show that the mean error obtained with the NOPERP protocol was higher than the mean error obtained with the REFOR protocol (in reference to the values obtained with the PERP protocol). However, probably because of the small size of our sample, this difference was not significant. Despite the different values obtained with the three protocols, there was a strong correlation between the volumes obtained by each method. This correlation between the three protocols explains the fact that the asymmetry indexes are not significantly modified by the protocol used.

In conclusion, the use of different protocols for measuring the volume of the hippocampal formation led to important variations in the absolute values of the calculated volumes. However, there was a strong correlation between the results obtained by each method. Consequently, any of the methods may be used to study a group of patients, but it is important to apply the same protocol throughout a given patient population. Moreover, if a preliminary study of control subjects is performed, it must also be done with the same protocol.

Acknowledgments

We thank Alessandra Biondi, MD, for helpful discussions in the revision of the manuscript, and Stéphan Blatrix, Carine Brunello, Cyrille Martinet, and Claire Savourat, the medical illustrators who created the original drawings.

References

1. Adam C, Baulac M, Saint-Hilaire J M, Landau J, Granat O, Laplane D. Value of magnetic resonance imaging-based measurements of hippocampal formations in patients with partial epilepsy. *Arch Neurol* 1994;51:130–138
2. Bronen RA. Epilepsy: the role of MR imaging. *AJR Am J Roentgenol* 1992;159:1165–1174
3. Cascino GD, Jack C Jr, Sharbrough FW, Kelly PJ, Marsh WR. MRI assessments of hippocampal pathology in extratemporal lesional epilepsy. *Neurology* 1993;43:2380–2382
4. Cendes F, Andermann F, Gloor P, et al. MRI volumetric measurement of amygdala and hippocampus in temporal lobe epilepsy. *Neurology* 1993;43:719–725
5. Cook MJ, Fish DR, Shorvon SD, Straughan K, Stevens JM. Hippocampal volumetric and morphometric studies in frontal and temporal lobe epilepsy. *Brain* 1992;115:1001–1015
6. Jack C Jr, Bentley MD, Twomey CK, Zinsmeister AR. MR imaging-based volume measurements of the hippocampal formation and anterior temporal lobe: validation studies. *Radiology* 1990; 176:205–209
7. Seab JP, Jagust WJ, Wong ST, Roos MS, Reed BR, Budinger TF. Quantitative NMR measurements of hippocampal atrophy in Alzheimer's disease. *Magn Reson Med* 1988;8:200–208

8. Press GA, Amaral DG, Squire LR. Hippocampal abnormalities in amnesic patients revealed by high-resolution magnetic resonance imaging. *Nature* 1989;341:54–57
9. Shenton ME, Kikinis R, Jolesz FA, et al. Abnormalities of the left temporal lobe and thought disorder in schizophrenia: a quantitative magnetic resonance imaging study. *N Engl J Med* 1992;327: 604–612
10. Suddath RL, Christison GW, Torrey EF, Casanova MF, Weinberger DR. Anatomical abnormalities in the brains of monozygotic twins discordant for schizophrenia. *N Engl J Med* 1990;322:789–794
11. Cascino GD, Jack C Jr, Parisi JE, et al. Magnetic resonance imaging-based volume studies in temporal lobe epilepsy: pathological correlations. *Ann Neurol* 1991;30:31–36
12. Cendes F, Andermann F, Dubeau F, et al. Early childhood prolonged febrile convulsions, atrophy and sclerosis of mesial structures, and temporal lobe epilepsy: an MRI volumetric study. *Neurology* 1993;43:1083–1087
13. Lencz T, McCarthy G, Bronen RA, et al. Quantitative magnetic resonance imaging in temporal lobe epilepsy: relationship to neuropathology and neuropsychological function. *Ann Neurol* 1992; 31:629–637
14. Jack CR. MRI-based hippocampal volume measurements in epilepsy. *Epilepsia* 1994;35:S21–S26
15. Kuks JB, Cook MJ, Fish DR, Stevens JM, Shorvon SD. Hippocampal sclerosis in epilepsy and childhood febrile seizures. *Lancet* 1993;342:1391–1394
16. Soininen HS, Partanen K, Pitkanen A, et al. Volumetric MRI analysis of the amygdala and the hippocampus in subjects with age-associated memory impairment: correlation to visual and verbal memory. *Neurology* 1994;44:1660–1668
17. Spencer SS, McCarthy G, Spencer DD. Diagnosis of medial temporal lobe seizure onset: relative specificity and sensitivity of quantitative MRI. *Neurology* 1993;43:2117–2124
18. Jack C Jr, Gehring DG, Sharbrough FW, Felmlee JP, Forbes G, Hench VS. Temporal lobe volume measurement from MR images: accuracy and left-right asymmetry in normal persons. *J Comput Assist Tomogr* 1988;12:21–29
19. Conlon P, Trimble MR, Rogers D, Callicott C. Magnetic resonance imaging in epilepsy: a controlled study. *Epilepsy Res* 1988;2: 37–43
20. White LE, Lucas G, Richards A, Purues D. Cerebral asymmetry and handedness. *Nature* 1994;368:197–198
21. Kuzniecky R, Burgard S, Faught E, Morawetz R, Bartolucci A. Predictive value of magnetic resonance imaging in temporal lobe epilepsy surgery. *Arch Neurol* 1993;50:65–69
22. Jackson GD, Berkovic SF, Duncan JS, Connelly A. Optimizing the diagnosis of hippocampal sclerosis using MR imaging. *AJNR Am J Neuroradiol* 1993;14:753–762
23. Squire LR, Amaral DG, Press GA. Magnetic resonance imaging of the hippocampal formation and mammillary nuclei distinguish medial temporal lobe and diencephalic amnesia. *J Neurosci* 1990; 10:3106–3117
24. Kesslak JP, Nalcioglu O, Cotman CW. Quantification of magnetic resonance scans for hippocampal and parahippocampal atrophy in Alzheimer's disease. *Neurology* 1991;41:51–54
25. Jack C Jr, Twomey CK, Zinsmeister AR, Sharbrough FW, Petersen RC, Cascino GD. Anterior temporal lobes and hippocampal formations: normative volumetric measurements from MR images in young adults. *Radiology* 1989;172:549–554
26. Ashtari M, Barr WB, Schaul N, Bogerts B. Three-dimensional fast low-angle shot imaging and computerized volume measurement of the hippocampus in patients with chronic epilepsy of the temporal lobe. *AJNR Am J Neuroradiol* 1991;12:941–947
27. Bhatia S, Bookheimer SY, Gaillard WD, Theodore WH. Measurement of whole temporal lobe and hippocampus for MR volumetry: normative data. *Neurology* 1993;43:2006–2010
28. Murro AM, Park YD, King DW, et al. Seizure localization in temporal lobe epilepsy: a comparison of scalp-sphenoidal EEG and volumetric MRI. *Neurology* 1993;43:2531–2533
29. Yoneda Y, Mori E, Yamashita H, Yamadori A. MRI volumetry of medial temporal lobe structures in amnesia following herpes simplex encephalitis. *Eur Neurol* 1994;34:243–252
30. Cendes F, Andermann F, Gloor P, et al. Atrophy of mesial structures in patients with temporal lobe epilepsy: cause or consequence of repeated seizures? *Ann Neurol* 1993;34:795–801
31. Jack CR Jr, Mullan DP, Sharbrough FW, et al. Intractable non lesional epilepsy of temporal lobe origin: lateralization by interictal SPECT versus MRI. *Neurology* 1994;44:829–836
32. Jack CR Jr, Krecke KN, Luetmer PH, et al. Diagnosis of mesial temporal sclerosis with conventional versus fast spin-echo MR imaging. *Radiology* 1994;192:123–127
33. Kim JH, Tien RD, Felsberg GJ, Osumi AK, Lee N. MR measurements of the hippocampus for lateralization of temporal lobe epilepsy: value of measurements of the body vs the whole structure. *AJR Am J Roentgenol* 1994;163:1453–1457
34. Tien RD, Felsberg GJ, Crain B. Normal anatomy of the hippocampus and adjacent temporal lobe: high-resolution fast spin-echo MR images in volunteers correlated with cadaveric histologic sections. *AJR Am J Roentgenol* 1992;159:1309–1313
35. Tien RD, Felsberg GJ, Campi de Castro C, et al. Complex partial seizures and mesial temporal sclerosis: evaluation with fast spin-echo MR imaging. *Radiology* 1993;189:835–842
36. Bathia S, Bookheimer SY, Gaillard WD, Theodore WH. Measurement of whole temporal lobe and hippocampus for MR volumetry: normative data. *Neurology* 1993;43:2006–2010
37. Ikeda M, Tanabe H, Nakagawa Y, et al. MRI-based quantitative assessment of the hippocampal region in very mild to moderate Alzheimer's disease. *Neuroradiology* 1994;36:7–10
38. Cendes F, Leproux F, Melanson D, et al. MRI of amygdala and hippocampus in temporal lobe epilepsy. *J Comput Assist Tomogr* 1993;17:206–210